Knockdown of cullin 3 inhibits progressive phenotypes and increases chemosensitivity in cholangiocarcinoma cells

KANDAWASRI PRATUMMANEE[1], KANKAMOL KERDKUMTHONG[1], SITTIRUK ROYTRAKUL[2], PHONPRAPAVEE TANTIMETTA[1], PHANTHIPHA RUNSAENG[1,3], SOMPOP SAEHENG[1,3] and SUMALEE OBCHOEI[1,3]

[1]Department of Biochemistry, Division of Health and Applied Sciences, Faculty of Science, Prince of Songkla University, Hatyai, Songkhla 90110, Thailand; [2]Functional Proteomics Technology Laboratory, National Center for Genetic Engineering and Biotechnology, National Science and Technology Development Agency, Pathumtani 12120, Thailand; [3]Center of Excellence for Biochemistry, Faculty of Science, Prince of Songkla University, Hatyai, Songkhla 90110, Thailand

Received May 28, 2024; Accepted August 8, 2024

DOI: 10.3892/mmr.2024.13322

Abstract. Cholangiocarcinoma (CCA) is an extremely aggressive malignancy arising from the epithelial cells lining the bile ducts. It presents a substantial global health issue, with the highest incidence rates, ranging from 40-100 cases/100,000 individuals, found in Southeast Asia, where liver fluke infection is endemic. In Europe and America, incidence rates range from 0.4-2 cases/100,000 individuals. Globally, mortality rates range from 0.2-2 deaths/100,000 person-years and are increasing in most countries. Chemotherapy is the primary treatment for advanced CCA due to limited options from late-stage diagnosis, but its efficacy is hindered by drug-resistant phenotypes. In a previous study, proteomics analysis of drug-resistant CCA cell lines (KKU-213A-FR and KKU-213A-GR) and the parental KKU-213A line identified cullin 3 (Cul3) as markedly overexpressed in drug-resistant cells. Cul3, a scaffold protein within CUL3-RING ubiquitin ligase complexes, is crucial for ubiquitination and proteasome degradation, yet its role in drug-resistant CCA remains to be elucidated. The present study aimed to elucidate the role of Cul3 in drug-resistant CCA cell lines. Reverse transcription-quantitative PCR and western blot analyses confirmed significantly elevated Cul3 mRNA and protein levels in drug-resistant cell lines compared with the parental control. Short interfering RNA-mediated Cul3 knockdown sensitized cells to 5-fluorouracil and gemcitabine and inhibited cell proliferation, colony formation, migration and invasion. In addition, Cul3 knockdown induced G_0/G_1 cell cycle arrest and suppressed key cell cycle regulatory proteins, cyclin D, cyclin-dependent kinase (CDK)4 and CDK6. Bioinformatics analysis of CCA patient samples using The Cancer Genome Atlas data revealed Cul3 upregulation in CCA tissues compared with normal bile duct tissues. STRING analysis of upregulated proteins in drug-resistant CCA cell lines identified a highly interactive Cul3 network, including COMM Domain Containing 3, Ariadne RBR E3 ubiquitin protein ligase 1, Egl nine homolog 1, Proteasome 26S Subunit Non-ATPase 13, DExH-box helicase 9 and small nuclear ribonucleoprotein polypeptide G, which showed a positive correlation with Cul3 in CCA tissues. Knocking down Cul3 significantly suppressed the mRNA expression of these genes, suggesting that Cul3 may act as an upstream regulator of them. Gene Ontology analysis revealed that the majority of these genes were categorized under binding function, metabolic process, cellular anatomical entity, protein-containing complex and protein-modifying enzyme. Taken together, these findings highlighted the biological and clinical significance of Cul3 in drug resistance and progression of CCA.

Correspondence to: Dr Sumalee Obchoei, Department of Biochemistry, Division of Health and Applied Sciences, Faculty of Science, Prince of Songkla University, 15 Karnjanavanich Road., Hatyai, Songkhla 90110, Thailand
E-mail: sumalee.o@psu.ac.th

Abbreviations: ARIH1, Ariadne RBR E3 ubiquitin protein ligase 1; CDK4/6, cyclin-dependent kinase 4/6; COMMD3, COMM Domain Containing 3; CRL3, CUL3-RING ubiquitin ligase; Cul3, cullin 3; DHX9, DExH-box helicase 9; DEPs, differentially expressed proteins; EGLN1, Egl nine homolog 1; EMT, epithelial-mesenchymal transition; LC-MS/MS, liquid chromatography with tandem mass spectrometry; PSMD13, Proteasome 26S Subunit Non-ATPase 13; SNRPG, small nuclear ribonucleoprotein polypeptide G

Key words: cholangiocarcinoma, cullin 3, drug resistance, 5-fluoruracil, gemcitabine

Introduction

Cholangiocarcinoma (CCA) is an aggressive cancer originating from the epithelial cells lining the biliary duct. Risk factors for CCA vary geographically, with primary sclerosing cholangitis identified as a prominent risk factor in western countries, while liver fluke infection predominates in Asian countries (1). The highest incidence rates, ranging from 40-100 cases/100,000 individuals, are found in areas endemic to liver fluke infection (2). In Europe and America, incidence

rates range from 0.4-2 cases/100,000 individuals (3). Globally, mortality rates are 0.2-2 deaths/100,000 person-years and are increasing in most countries (4). In the early stages, CCA often presents asymptomatically, leading to late-stage diagnosis, which results in a poor prognosis and limited treatment options. Consequently, most patients are not suitable candidates for curative surgery and advanced cases necessitate palliative treatments combined with radiotherapy or chemotherapy (5,6). However, these treatments marginally extend survival, with rates typically below one year (7-9). Drug resistance in cancer cells significantly contributes to treatment ineffectiveness and recurrence (10), underscoring the urgent need for novel prognostic biomarkers or therapeutic targets to overcome drug resistance in CCA.

Cullin proteins serve as molecular scaffolds within Cullin-RING ubiquitin ligase (CRL) complexes (11), which are crucial for the post-translational modification of cellular proteins through ubiquitination. They can undergo a post-translational modification called neddylation, which involves the covalent attachment of a protein called neural precursor cell expressed developmentally downregulated protein 8 (NEDD8) to a lysine residue of a protein substrate. Cullins are the best-characterized physiological substrates of neddylation. This modification is catalyzed by an enzyme cascade consisting of the NEDD8 activating enzyme, NEDD8 conjugating enzyme (E2) and NEDD8 ligase [ubiquitin protein ligase 1 (E3)] (12). Neddylation of cullins leads to the activation of CRLs, thereby controlling the ubiquitination of cellular proteins (13). Cullin 3 (Cul3), encoded by the *CUL3* gene, acts as a scaffold protein within CUL3-RING ubiquitin ligase (CRL3) complexes, pivotal for various cellular processes, including protein degradation, cell cycle regulation, DNA damage repair and epigenetic modulation (14). Emerging evidence implicates Cul3 in tumorigenesis and tumor progression through the degradation of oncoproteins or tumor suppressor proteins (15). For instance, Cul3 may play a direct role in the proteasomal degradation of adhesion-associated cytoskeletal proteins and metastasis suppressor proteins, potentially regulating metastasis in both breast (16) and bladder cancer (17). In addition, Cul3 expression in bladder cancer positively correlates with tumor stages and disease-free survival. In prostate cancer, hypoxia plays a critical role in advancing the disease and fostering resistance to treatments. Cul3, along with its substrate adaptor protein Kelch-Like Family Member 20, facilitates the breakdown of Promyelocytic Leukemia Protein. This affects the hypoxia-inducible factor 1 signaling pathway, which in turn drives tumor progression and resistance to chemotherapy (18). Conversely, Cul3 is a good prognostic marker in lung adenocarcinoma, where it seems to act as a tumor suppressor. Forced overexpression of Cul3 attenuates tumor progression through its interaction with Kelch-like ECH-associated protein 1 and the subsequent regulation of the Nrf2/RhoA axis (19). While the involvement of Cul3 in tumorigenesis, either as an oncogene or tumor suppressor gene, has been proposed in various cancers, its role in tumor progression and drug resistance in CCA is largely unexplored.

Previously, our research group established 5-fluorouracil- and gemcitabine-resistant CCA cell lines, designated KKU-213A-FR and KKU-213A-GR, respectively (20). Subsequent proteomic analysis revealed the upregulation of numerous proteins, including Cul3, in drug-resistant cells. The present study confirmed elevated Cul3 expression at both mRNA and protein levels in these drug-resistant CCA cell lines. Furthermore, it investigated the effect of short interfering (si)RNA-mediated Cul3 knockdown on cell proliferation, colony formation, cell motility and drug sensitivity. The clinical relevance of Cul3 was explored through online databases and bioinformatics analyses.

Materials and methods

Cell culture. The human CCA cell line, KKU-213A, was obtained from the Japanese Collection of Research Bioresources Cell Bank in Osaka, Japan. The drug-resistant cell lines were previously established by our research group. High-glucose Dulbecco's Modified Eagle's Medium (DMEM) supplemented with 10% fetal bovine serum (FBS) (Gibco; Thermo Fisher Scientific, Inc.) and 1% antibiotic-antimycotic mixture (Gibco; Thermo Fisher Scientific, Inc.) was used as the culture medium for maintaining all cell lines throughout the present study. All cell lines were cultured at 37˚C with 5% CO_2 and saturated humidity.

Drug-resistant CCA cell lines. The drug-resistant CCA cell lines designated KKU-213A-FR and KKU-213A-GR, were established by exposing the parental cell line KKU-213A to gradually increasing concentrations of the commonly used chemotherapeutic drugs 5-fluorouracil (5-FU) and gemcitabine, as previously described (21,22). In brief, KKU-213A was cultured in DMEM containing the IC_{25} concentrations of each chemotherapeutic drug. The drug concentration was then gradually increased until the cell lines could grow exponentially in the presence of the desired chemotherapeutic drug, 7 μM 5-FU or 3 μM gemcitabine.

Proteomics analysis using liquid chromatography with tandem mass spectrometry (LC-MS/MS). Previously, proteomic analysis was performed using LC-MS/MS to compare KKU-213A, KKU-213A-FR and KKU-213A-GR cell lines. In brief, cell pellets were lysed with 0.5% sodium dodecyl sulfate (SDS) and then centrifuged at 10,000 x g for 15 min at 4˚C to collect the protein supernatant. The protein was precipitated with two volumes of cold acetone and incubated at -20˚C overnight. The mixture was then thawed, centrifuged and the supernatant was discarded. The pellet was dried and preserved at -80˚C. For LC-MS/MS, all protein samples were digested with trypsin at a 1:20 ratio for 16 h at 37˚C before being introduced into an Ultimate3000 Nano/Capillary LC System (Thermo Fisher Scientific, Inc.), connected to an HCTUltra LC-MS system (Bruker Daltonics; Bruker Corporation), equipped with a nano-captive spray ion source. The data obtained from LC-MS were analyzed using DecyderMS 2.0 Differential Analysis software (23,24) with the human protein database from UniProt (version 2021_03; http://www.uniprot.org/). The search parameters allowed for a maximum of three missed cleavages. The MS proteomics data were deposited in the ProteomeXchange Consortium via the jPOST partner repository with the dataset identifier JPST002506 and PXD049309 (https://proteomecentral.proteomexchange.org/cgi/GetDataset?ID=PXD049309). Proteins that demonstrated >3-fold variation in KKU-213A-FR and KKU-213A-GR

expression compared with the parental cell line, with a False Discovery Rate (FDR) of <0.05, were identified as differentially expressed proteins (DEPs).

siRNAs and transfection. To knock down Cul3 expression in drug-resistant CCA cells, KKU-213A-FR and KKU-213A-GR were plated at $2x10^5$ cells/well in a 6-well plate and incubated for 24 h. siRNAs targeting Cul3 mRNA (siCul3#1 and siCul3#2) and a negative control siRNA (siNC) were obtained from Gene Universal (Gene Universal Inc.). The sequences were: siCul3#1, 5'-ACCUGAUGAUUCUUGGAUATT-3'; siCul3#2, 5'-GUGUAAUUCUCUGCCUUCATT-3'; siNC, 5'-UUCUCCGAACGUGUCACGUTT-3'. The siRNAs, at a final concentration of 100 μM, were transfected into the cells using Lipofectamine® 2000 (Invitrogen; Thermo Fisher Scientific, Inc.) as the transfection reagent, following the manufacturer's instructions. The cells were incubated with the transfection complex for 6 h at 37˚C in a CO_2 incubator, then switched to complete medium and further incubated for 24-48 h, depending on the subsequent experiments. Cells for RNA and protein extractions were harvested after a 48-h incubation, while for other phenotypic studies, the transfected cells were harvested after 24 h of incubation.

Reverse transcription-quantitative (RT-q) PCR. Total RNA was extracted from the cells using TRIzol™ Reagent (Thermo Fisher Scientific, Inc.) and subsequently converted into cDNA using the RevertAid First Strand cDNA Synthesis Kit (Thermo Fisher Scientific, Inc.). Quantitative real-time PCR analysis was performed with the PanGreen Universal SYBR Green Master Mix (2X) (Bio-Helix Co., Ltd.). RNA extraction, cDNA synthesis and qPCR were carried out according to the manufacturer's protocols. β-actin was used as the internal control and the primer sequences are provided in Table I. The thermal cycling conditions were as follows: Initial denaturation at 95˚C for 15 min, denaturation at 95˚C for 20 sec, annealing at 60˚C for 1 min, and extension at 72˚C for 2 min, followed by 35 cycles of denaturation and annealing. The relative expression levels were calculated using the $2^{-\Delta\Delta Cq}$ method (25).

Cell proliferation assay. Cell proliferation was examined using the 3-[4,5-dimethyl thiazole-2-yl]-2,5-diphenyl-tetrazolium bromide (MTT) assay. MTT was purchased from MilliporeSigma. The KKU-213A-FR and KKU-213A-GR cell lines, transfected with siNC, siCul3#1, or siCul3#2, were seeded at $1.5x10^3$ cells/well in a 96-well plate and incubated for 12, 24, 48 and 72 h. Then, 0.5 mg/ml MTT was added to each well and incubated for 2 h at 37˚C. After discarding the excess MTT solution, 100 μl DMSO was added to dissolve the formazan crystals. The intensity of solubilized formazan was recorded as absorbance at 540 nm using a microplate reader (Spark multimode microplate reader; Tecan Group, Ltd.). The cell growth rate was calculated as a fold change of absorbance compared with the 12-h time point. The difference in growth rate was then compared between the siNC and siCul3#1 groups and between the siNC and siCul3#2 groups at each time point.

Chemotherapeutic drug sensitivity assay. To confirm the drug-resistant phenotype of the established cell line and to assess whether knockdown of Cul3 in the KKU-213A-FR and KKU-213A-GR cells can reverse this phenotype, a chemotherapeutic drug sensitivity assay was performed. The parental and drug-resistant cells, as well as the siNC transfected and siCul3 transfected cells, were seeded at $1.5x10^3$ cells per well into each well of a 96-well plate and incubated overnight. The next day, the culture medium was replaced with various concentrations of 5-FU (0, 3.125, 6.25, 12.5 and 25 μM; MilliporeSigma) or gemcitabine (0, 1.25, 2.5, 5 and 10 μM; MilliporeSigma) and incubated for another 72 h. The remaining cells were estimated using an MTT assay as aforementioned. The percentage of remaining cells for each treatment was calculated by comparing to the untreated control, considered as 100% cell viability. The percentage of remaining cells at each drug concentration was then compared between KKU-213A and KKU-213A-FR, KKU-213A and KKU-213A-GR, the siNC and siCul3#1 groups and the siNC and siCul3#2 groups.

Table I. List of primers.

Gene		Sequence (5'→3')
CUL3	Forward:	GTTCGATCGCTTCCTCCTGG
	Reverse:	AGGAGACCTGGAGTTGAGGTT
ARIH1	Forward:	TGCGCCTGATCACAGATTCA
	Reverse:	CACATTTGCAGCGAACAGGT
COMMD3	Forward:	TAGAGGCAGGAAAGCACCGA
	Reverse:	AAGCGCCAAGAAACATCCGT
DHX9	Forward:	GTACGGCCTGGATTCTGCTT
	Reverse:	ATCACAGCATCCAAAGGGGG
EGLN1	Forward:	GAGAAGGCGAACCTGTACCC
	Reverse:	CACAGATGCCGTGCTTGTTC
PSMD13	Forward:	ACCTTCCTGGTGTGACATCG
	Reverse:	CCCAAAAACCGCAGAGCATC
SNRPG	Forward:	GGTGGCAGACATGTCCAAGG
	Reverse:	CCATTCCAATATTGTTCTGTTG
β-actin	Forward:	GGATTCCTATGTGGGCGACG
	Reverse:	TTGTAGAAGGTGTGGTGCCAG

Colony formation assay. To evaluate the effect of Cul3 knockdown on the ability of cells to grow from a single cell, a colony formation assay was performed. Briefly, transfected cells were harvested via trypsinization, counted and dispersed into single cells. A low concentration of cells (500 cells/ml) was then seeded into a 6-well plate and incubated for 14 days, with the medium changed every 3-4 days. Upon completion, the colonies were fixed with 4% paraformaldehyde at room temperature for 15 min and stained with 0.4% sulforhodamine B (SRB) solution at room temperature for 10 min. After the excess dye was removed, the plate was washed, dried and the number of colonies was counted. Colonies were defined as cell clusters with a diameter of at least 0.5 mm. Colony numbers were compared between the siCul3 and siNC groups.

Cell migration and invasion assays. The cell migration and invasion capabilities were investigated using a modified Boyden chamber technique. After transfection with siRNAs, cells were trypsinized and resuspended in serum-free medium. Then,

200 μl of the cell suspension containing $4x10^4$ cells was seeded onto the Transwell insert with an 8-μm porous polycarbonate membrane (Corning Life Sciences) and the lower chamber was filled with complete medium. For cell invasion assays, the membrane was pre-coated with 0.5 mg/ml Matrigel (Corning Life Sciences) for 2 h at 37˚C prior to cell seeding. Cells were allowed to migrate or invade through the porous membrane for 11 h. After that, the non-migrated and non-invaded cells on the upper part of the Transwell insert were removed with a cotton swab. The membrane was then fixed with 4% paraformaldehyde at room temperature for 15 min and stained with 0.4% SRB solution at room temperature for 10 min. Images were captured at 100x magnification using an inverted light microscope (Olympus CKX53; Olympus Corporation), and cells from five randomly selected low-power fields were counted using ImageJ software (version 1.53t; National Institutes of Health).

Cell cycle analysis. The effect of Cul3 suppression on cell cycle distribution was analyzed through flow cytometric analysis. Briefly, the transfected cells were harvested and fixed with 70% ethanol and incubated on ice for 30 min. The cells were washed twice with phosphate-buffered saline (PBS) and then stained with a DNA staining solution containing propidium iodide (PI; 50 μg/ml), RNase A (100 μg/ml), Triton X-100 (0.1%) and EDTA (0.1 mM) for 15 min. The cell cycle analysis was carried out using the Attune NxT Flow Cytometer (Thermo Fisher Scientific, Inc.) and the results obtained from three independent experiments were analyzed with FCS Express 7 (De Novo Software).

Western blotting. Proteins were extracted from parental, drug-resistant CCA cell lines and siRNA-transfected cells using RIPA lysis buffer (Visual Protein) with a protease inhibitor cocktail (Merck KGaA). Protein concentration was determined using a bicinchoninic acid (BCA) protein assay kit (Bio Basic Inc.) according to the manufacturer's instructions. Equal amounts of protein (30 μg) from different samples were separated on 12% SDS-PAGE via electrophoresis and transferred to Hybond-PVDF membranes (Cytiva). After blocking the membranes with 5% skimmed milk at room temperature for 1 h, the membranes were incubated at 4˚C overnight with primary antibodies against Cul3, cyclin D, cyclin-dependent kinase (CDK)4, CDK6, or β-actin. The membranes were washed three times and subsequently incubated with a horseradish peroxidase (HRP)-linked secondary antibody at room temperature for 1 h. Detailed information and dilutions of the antibodies are presented in Table II. Finally, the signal of protein bands was developed using SuperSignal West Pico PLUS Chemiluminescent Substrate (Thermo Fisher Scientific, Inc.) and captured by an Alliance Q9-ATOM Chemiluminescent Imaging System (Uvitec Ltd.). Relative band intensity was analyzed using ImageJ software (version 1.53t; National Institutes of Health).

Bioinformatics analysis. To assess the aberrant mRNA expression of Cul3 in the tissues of patients with CCA based on sample types and tumor metastasis status, the University of Alabama at Birmingham Cancer (UALCAN) web portal (https://ualcan.path.uab.edu/) (26) was used. This platform obtained data from The Cancer Genome Atlas (TCGA) project, allowing users to evaluate protein-coding gene expression and its clinical significance across 33 types of cancer.

To evaluate the prognostic potential of Cul3 in CCA, overall survival (OS) and disease-free survival (DFS) analyses was performed using the Gene Expression Profiling Interactive Analysis 2 (GEPIA2) tool (http://gepia2.cancer-pku.cn/) (27). Kaplan-Meier survival plots were generated to illustrate the association between Cul3 expression and OS or DFS, with P-values from the log-rank test considered statistically significant if less than 0.05. In addition, GEPIA2 was employed to assess the correlation between Cul3 and its associated genes (*ARIH1*, *COMMD3*, *EGLN1*, *PSMD13*, *DHX9* and *SNRPG*). The correlations were computed using Pearson correlation coefficients and presented in scatter plots. $P<0.05$ was considered to indicate a statistically significant difference.

Protein expression levels of Cul3 in CCA and normal bile duct tissues were obtained from The Human Protein Atlas (HPA; https://proteinatlas.org/). The HPA is a comprehensive database containing immunohistochemistry (IHC)-based protein expression profiles in cancer tissues, normal tissues and cell lines (28). IHC images from six tumor tissues and three normal tissues were downloaded from the HPA. The staining intensity of these IHC images was analyzed using ImageJ software (version 1.53t; National Institutes of Health). The Search Tool for the Retrieval of Interacting Genes/Proteins (STRING) database (https://string-db.org/) (29) was used to perform a comprehensive analysis of the protein-protein interactions (PPI) involving Cul3-associated proteins.

Cul3 and its correlated genes were classified using the Protein Analysis Through Evolutionary Relationships (PANTHER) classification system (version 19.0; https://www.pantherdb.org/) based on Gene Ontology (GO) annotations (30), with *Homo sapiens* as the reference organism. The organizational chart for proteins, classified based on their gene IDs and functional classification hits, is depicted graphically. Subsequently, these proteins were categorized according to molecular function, biological process, cellular component and protein class, with unclassified proteins filtered out. The Kyoto Encyclopedia of Genes and Genomes (KEGG) serves as a predictive tool for molecular networks between Cul3 and its correlated genes in various pathways. The present study used ShinyGO 0.80 (http://bioinformatics.sdstate.edu/go/), which is based on the KEGG pathways (31), to analyze the relationships between these genes. Parameters such as an FDR cutoff of 0.05 and a minimum pathway size of two genes were selected. The maximum pathway size was set at seven genes and redundant and abbreviated pathways were removed to show a total of 100 pathways.

Statistical analysis. Results are presented as mean ± standard deviation (SD). For comparisons between two groups, paired two-tailed Student's t-tests were conducted. For comparisons among three groups, one-way ANOVA was used; if significant differences were found, a Scheffe post hoc test was then applied. Correlations between Cul3 and other genes were analyzed using the Pearson correlation coefficient (R). Patient survival analysis was performed using Kaplan-Meier plots and the significance of survival differences was assessed with the log-rank test. Welch's t-test was used to evaluate the significance of differences in expression levels between normal and

Table II. List of antibodies.

Antibody	Host	Catalogue number	Dilution	Manufacturer
Anti-Cul3	Rabbit	2759	1:5,000	Cell Signaling Technology, Inc.
Anti-β-actin	Mouse	A5411	1:10,000	MilliporeSigma
Anti-cyclin D	Mouse	2936	1:2,500	Cell Signaling Technology, Inc.
Anti-CDK4	Rabbit	12790	1:2,500	Cell Signaling Technology, Inc.
Anti-CDK6	Mouse	3136	1:2,500	Cell Signaling Technology, Inc.
HPR-linked anti-Rabbit IgG	Goat	ab6721	1:10,000	Abcam
HPR-linked anti-Mouse IgG	Goat	ab6789	1:10,000	Abcam

tumor tissues. For comparisons among three groups [normal, tumor subgroup without nodule metastasis (N0) and tumor subgroup with metastases in 1-3 axillary lymph nodes (N1)], Welch's ANOVA was applied followed by Dunnett's T3 test. Each experiment was conducted with at least three replicates. $P<0.05$ was considered to indicate a statistically significant difference.

Results

Cul3 is highly expressed in drug-resistant CCA cell lines. The drug-resistant phenotypes of the previously established drug-resistant CCA cell lines were confirmed using the MTT assay. The results showed that at various concentrations of the chemotherapeutic drugs used, the cell viability of the drug-resistant cells was significantly higher than that of their parental counterparts in both KKU-213A-FR (Fig. 1A and Table SI) and KKU-213A-GR (Fig. 1B and Table SI). Previously, our research group conducted proteomics analysis on drug-resistant CCA cell lines (KKU-213A-FR and KKU-213A-GR) compared with their parental cell line (KKU-213A). Cul3 is one of the differentially expressed proteins highly expressed in both drug-resistant cell lines compared with parental control cells (Fig. 1C). The present study first confirmed the expression of Cul3 mRNA and protein using RT-qPCR and western blotting, respectively, in KKU-213A-FR and KKU-213A-GR, along with the parental cell line KKU-213A. The results showed that mRNA expression in both drug-resistant cell lines was more than 2-fold higher than in the parental cells (Fig. 1D and Table SI). Similarly, western blotting results demonstrated a ~2-fold higher expression of Cul3 protein in both drug-resistant cells compared with the parental control (Fig. 1E and Table SI). There are two bands of Cul3 at ~82 and 84 kDa, representing the non-neddylated and neddylated forms of Cul3, respectively.

siRNA-mediated knockdown of Cul3. To explore the significant role of Cul3 in CCA progression, specific siRNAs targeting Cul3 mRNA were transfected into KKU-213A-FR and KKU-213A-GR cells. Cells transfected with siNC were used as controls in all experiments. At 24 h post-transfection, the knockdown efficiency was assessed by RT-qPCR and western blotting. The results indicated that both siRNA strands effectively suppressed Cul3 expression. Cul3 mRNA was suppressed by siCul3#1 to 38 and 59% and by siCul3#2 to 35 and 50% in KKU-213A-FR and KKU-213A-GR, respectively (Fig. 1F and Table SI). Western blotting results showed that siCul3#1 suppressed Cul3 protein levels to 50 and 59% and siCul3#2 to 35 and 33% in KKU-213A-FR and KKU-213A-GR, respectively (Fig. 1G and Table SI).

Cul3 silencing enhances chemosensitivity. As Cul3 was observed to be elevated in drug-resistant CCA cells, it was hypothesized that suppressing Cul3 expression might render KKU-213A-FR and KKU-213A-GR cells more sensitive to chemotherapeutic drugs. MTT assay demonstrated that the cell viability of siCul3#1- and siCul3#2-transfected KKU-213A-FR and KKU-213A-GR cells significantly decreased upon treatment with 5-FU and gemcitabine, respectively, compared with cells transfected with siNC (Fig. 2A and Table SII), suggesting that Cul3 knockdown increased the chemosensitivity of drug-resistant cells. In addition, it was observed that siCul3#1 was more efficient than siCul3#2 in suppressing the drug-resistant phenotype of CCA cells.

Cul3 knockdown inhibits aggressive phenotypes of drug-resistant CCA cells. The aggressive phenotypes of the cells, including cell growth rate, ability to grow from a single cell to form a colony and cell motility, were assessed after Cul3 knockdown using MTT, colony formation and modified Boyden chamber assays, respectively. The MTT results showed that the growth rate of KKU-213A-FR and KKU-213A-GR cells following Cul3 silencing with both strands of siRNA significantly decreased at 48 and 72 h compared with controls (Fig. 2B and Table SII). The colony formation assay results demonstrated that the downregulation of Cul3 significantly reduced the number of colonies in KKU-213A-FR and KKU-213A-GR cells (Fig. 2C and Table SII). Furthermore, cell migration and invasion assays using the modified Boyden chamber revealed that suppression of Cul3 expression attenuated cell motility in both drug-resistant CCA cell lines (Fig. 2D and Table SII). Taken together, these results indicated that knockdown of Cul3 suppressed the aggressive phenotypes of drug-resistant CCA cell lines. It was observed that siCul3#1 was more efficient than siCul3#2 in suppressing cell growth and colony formation of CCA cells. However, the same phenomenon was not observed in cell migration and cell invasion. This may be caused by several factors, such as the duration of the experiments. For the cell migration and invasion assays, the cells were allowed to migrate

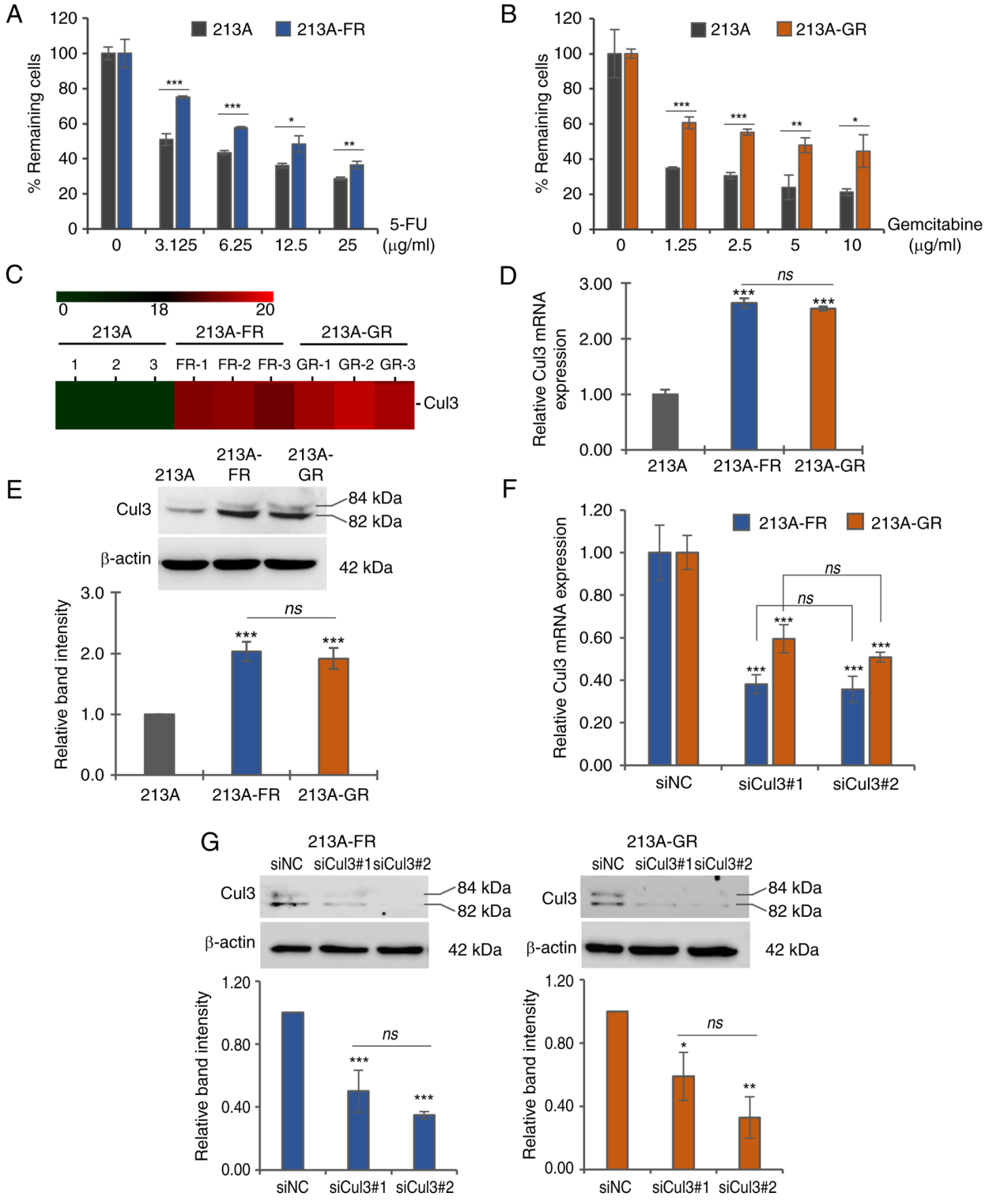

Figure 1. Cul3 mRNA and protein expression and siRNA-mediated knockdown of Cul3 in drug-resistant CCA cells. Drug sensitivity assay using the MTT test to confirm the drug-resistant phenotype of (A) KKU-213A-FR and (B) KKU-213A-GR. (C) Heat map representing Cul3 protein expression in drug-resistant CCA cell lines compared with the parental cell line. (D) mRNA expression of Cul3 in parental and drug-resistant CCA cell lines verified by RT-qPCR. (E) Cul3 protein expression in cell lines determined by western blotting. Cul3 was knocked down using siRNAs in KKU-213A-FR and KKU-213A-GR and knockdown efficiency was confirmed at both (F) the mRNA level by RT-qPCR and (G) the protein level by western blotting. Data are presented as mean ± standard deviation from three replicates. Significant differences between parental vs. drug-resistant cells or between siNC-vs. siCul3-transfected groups are indicated by *P<0.05, **P<0.01 and ***P<0.001; Cul3, cullin 3; si, short interfering; CCA, cholangiocarcinoma; MTT, 3-[4,5-dimethyl thiazole-2-yl]-2,5-diphenyl-tetrazolium bromide; RT-qPCR, reverse transcription-quantitative PCR; ns, not significant.

and invade for only 11 h, whereas other experiments, such as drug sensitivity and cell growth assays, were conducted over a longer period (e.g., 72 h for drug sensitivity and cell growth assays and 2 weeks for the colony formation assay). In addition, when statistical analyses were performed comparing siCul3#1 and siCul3#2 on the suppression of cell migration

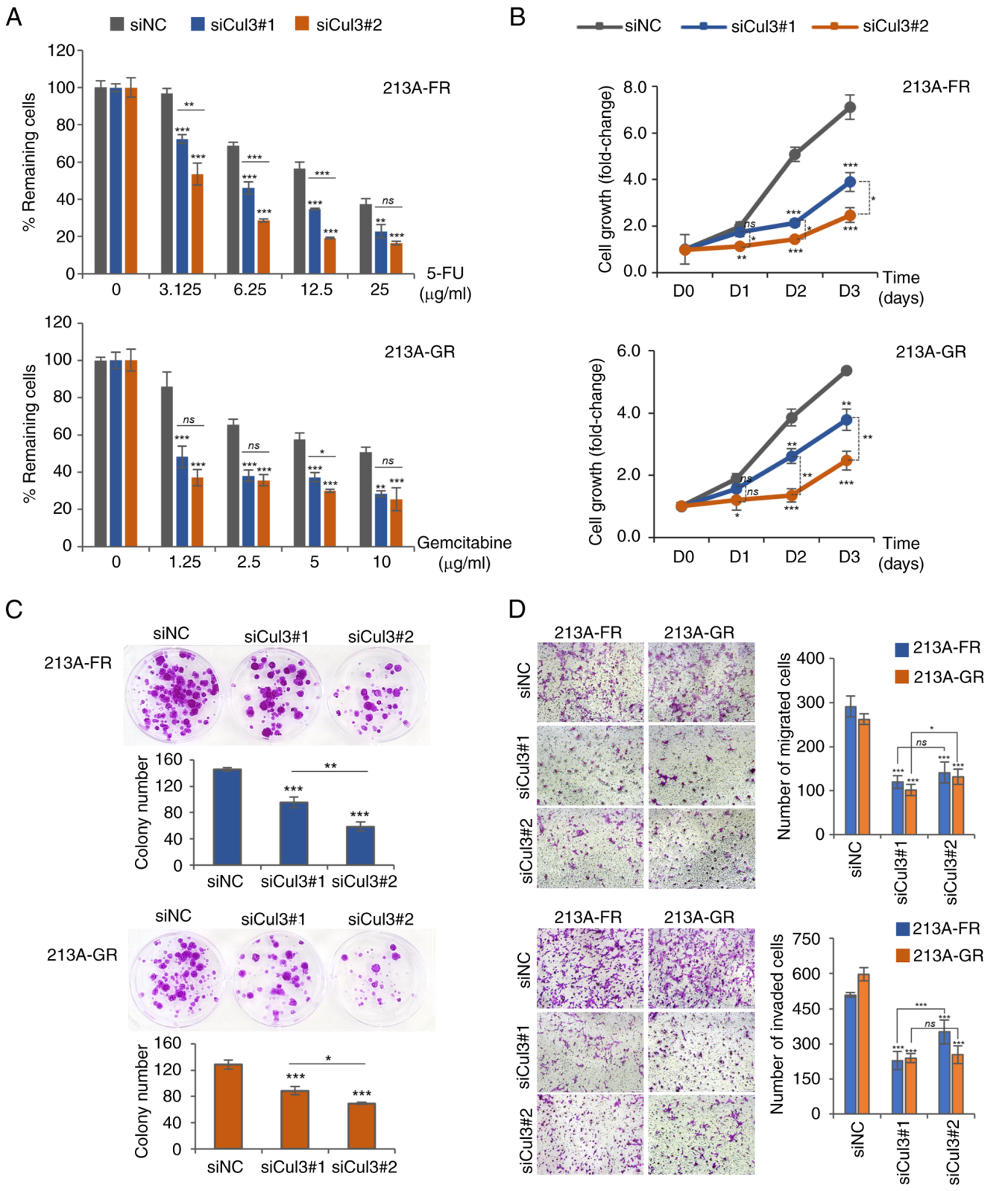

Figure 2. Cul3 knockdown attenuates drug-resistant and progressive phenotypes of CCA cells. (A) Drug sensitivity assay using MTT. (B) Cell growth assay using MTT. (C) Colony formation assay. (D) Cell migration and invasion assay using the modified Boyden chamber method (magnification, 100x). Data are presented as mean ± standard deviation from three replicates. Significant differences between siNC- and siCul3-transfected groups are indicated by *P<0.05, **P<0.01 and ***P<0.001. Cul3, cullin 3; CCA, cholangiocarcinoma; MTT, 3-[4,5-dimethyl thiazole-2-yl]-2,5-diphenyl-tetrazolium bromide; si, short interfering; NC, negative control; ns, not significant.

and invasion, it found the following: for KKU-213A-FR, cell migration (ns, P=0.299) and cell invasion (***P=0.008); and for KKU-213A-GR, cell migration (*P=0.017) and cell invasion (ns, P=0.711). These differences are not substantial and may be due to the short duration of the assays and small variations during the experiments.

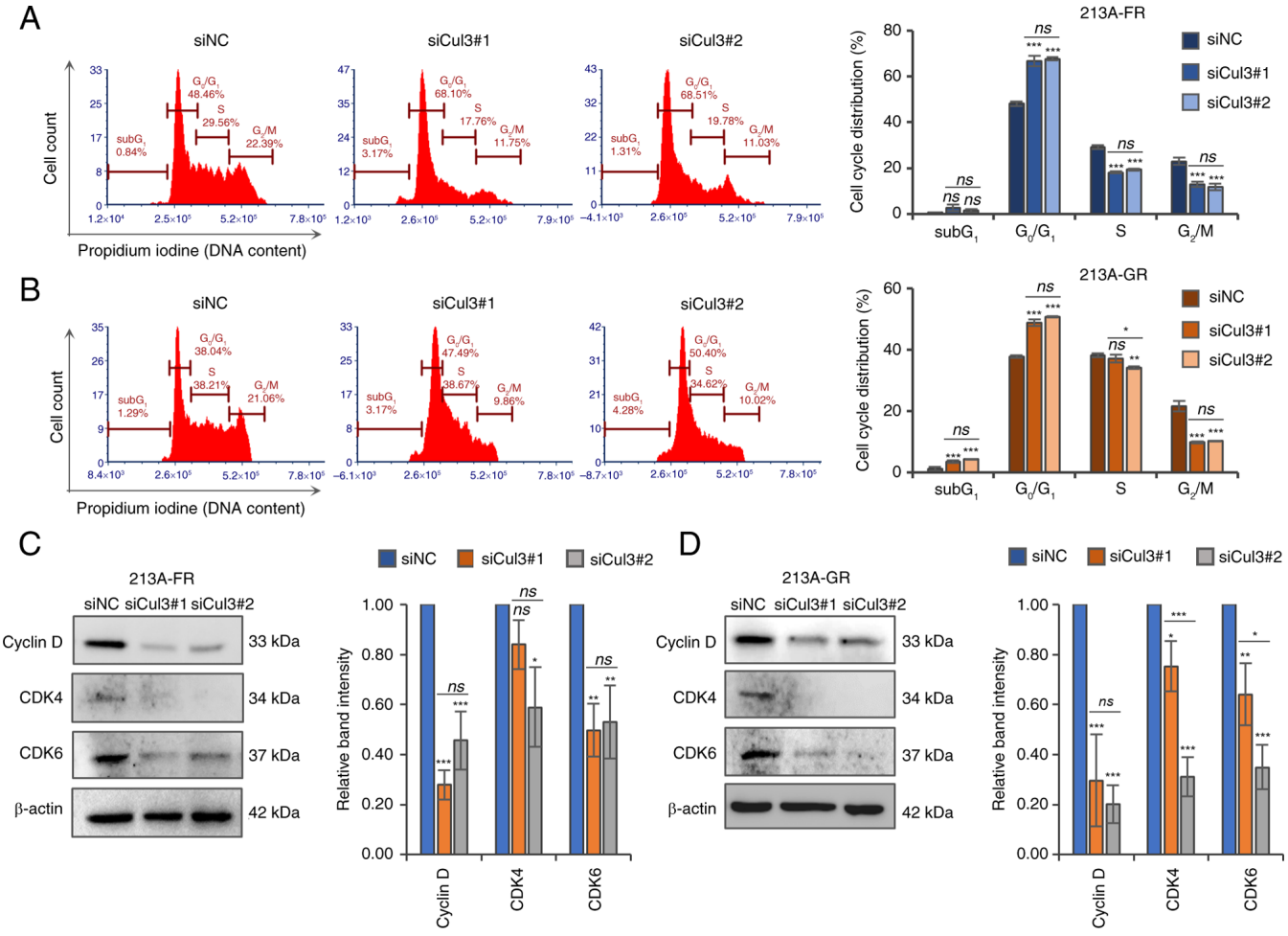

Figure 3. Knockdown of Cul3 induces G_0/G_1 cell cycle arrest in drug-resistant CCA cells. Cell cycle distribution was analyzed using propidium iodide staining and flow cytometric analysis in (A) KKU-213A-FR and (B) KKU-213A-GR cells. Cell cycle regulatory proteins, cyclin D, CDK4 and CDK6, were determined using western blotting in (C) KKU-213A-FR and (D) KKU-213A-GR cells. Representative blots and bar graphs show relative band intensity analyzed by ImageJ software. Data are presented as mean ± standard deviation from three replicates. Significant differences between parental vs. drug-resistant cells or between siNC-vs. siCul3-transfected groups are indicated by *P<0.05, **P<0.01 and ***P<0.001. Cul3, cullin 3; CCA, cholangiocarcinoma; CDK, cyclin-dependent kinase; si, short interfering; NC, negative control; ns, not significant.

Silencing of Cul3 induces G_0/G_1 cell cycle arrest. As Cul3 knockdown negatively affected cell growth (Fig. 2B), the effect of suppressing Cul3 expression on cell cycle distribution was further investigated. siRNA- and siNC-transfected cells were subjected to DNA staining with propidium iodide followed by flow cytometric analysis. The cell cycle distribution results showed that the percentage of cells in the G_0/G_1 phase significantly increased, while the number of cells in the G_2/M phases significantly decreased in Cul3 knockdown cells in both KKU-213A-FR (Fig. 3A and Table SIII) and KKU-213A-GR (Fig. 3B and Table SIII) cell lines. In addition, the proportion of cells in the S phase significantly decreased in KKU-213A-FR cells, whereas only a slight change was observed in KKU-213A-GR cells, following Cul3 knockdown. Next, the expression of key cell cycle regulatory proteins of the G_1 phase was determined using western blotting. The results demonstrated that cyclin D, CDK4 and CDK6 were significantly decreased in Cul3 knockdown KKU-213A-FR (Fig. 3C and Table SIII) and KKU-213A-GR (Fig. 3D and Table SIII) cells. The expression level of CDK4 protein was significantly suppressed by siCul3#2 in both cell lines but was only slightly suppressed by siCul3#1, with the reduction in KKU-213A-FR not being significant. These results suggested that Cul3 silencing suppresses cell growth partly by reducing cyclin D, CDK4 and CDK6 expression, resulting in cell cycle arrest at the G_0/G_1 phases.

Cul3 is upregulated in CCA tissues of patients. To investigate the clinical relevance of Cul3, the correlation between Cul3 mRNA expression and data of patients with CCA from the TCGA database was analyzed using the UALCAN web portal. The results revealed that Cul3 mRNA was highly expressed in tumor tissues, while its expression level was low in normal bile duct tissues (Fig. 4A). Since lymph node metastasis is one of the most important prognostic factors in numerous cancers, TCGA data based on lymph node metastasis status (N) was analyzed. The N category, part of the Tumor, Node, Metastasis (TNM) system, refers to the lymph node status: N0, no regional lymph node metastasis; N1, metastases in 1 to 3 axillary lymph nodes; N2, metastases in 4 to 9 axillary lymph nodes; and N3, metastases in 10 or

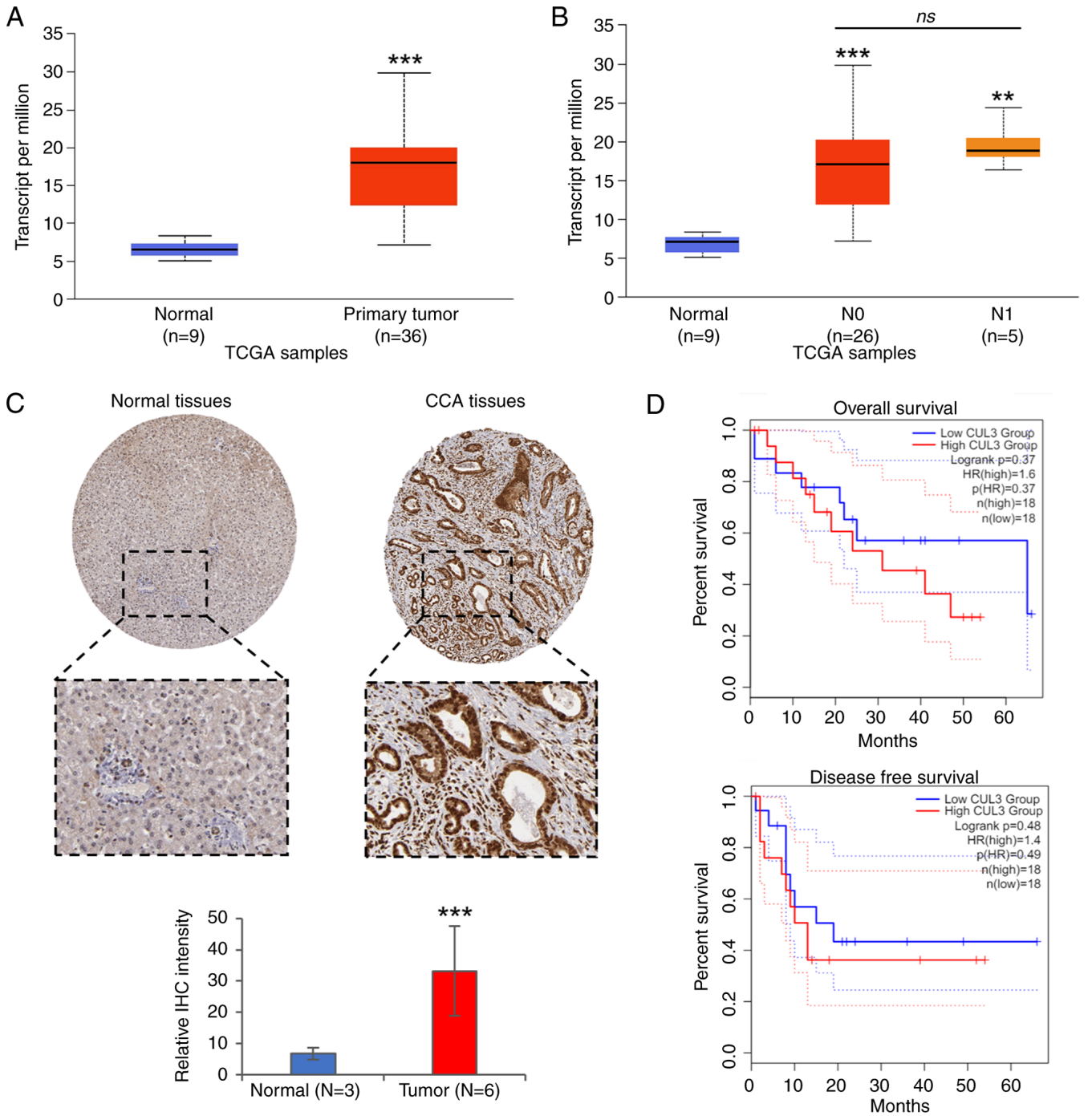

Figure 4. Cul3 expression in CCA patients' tissues. (A) mRNA expression of Cul3 in CCA patients' tissues analyzed through the UALCAN platform based on TCGA data. Red box: Cul3 mRNA expression level in tumor tissues (n=36); blue box: Cul3 mRNA expression level in normal bile duct tissues (n=9). (B) Cul3 mRNA expression analyzed based on lymph node metastasis status. Red box: Cul3 mRNA expression in patients with no regional lymph node metastasis (n=26); orange box: Cul3 mRNA expression in patients with tumor metastasized to 1 to 3 axillary lymph nodes (n=5); blue box: Cul3 mRNA expression level in normal bile duct tissues (n=9). (C) Representative images of Cul3 protein expression determined by immunohistochemistry staining in tumor and normal bile duct tissues, obtained from the Human Protein Atlas database (magnification, 40x). Bar graphs represent relative immunohistochemistry staining intensity in each group. (D) Overall survival and disease-free survival analysis of Cul3 expression levels in CCA patients. Significant differences between normal and tumor groups, normal and N0 groups or normal and N1 groups are indicated by **P<0.01 and ***P<0.001. Cul3, cullin 3; CCA, cholangiocarcinoma; IHC, immunohistochemistry; TCGA, The Cancer Genome Atlas; UALCAN, the University of Alabama at Birmingham Cancer; ns, not significant.

more axillary lymph nodes. When analyzed based on lymph node metastasis status, Cul3 expression was slightly higher in the metastasis group (N1) compared with the non-lymph node metastasis group (N0); however, this difference was not significant (Fig. 4B). In this dataset, N2, N3 and N4 groups were not available for analysis. The protein expression of Cul3, determined by immunohistochemistry staining, was obtained from The Human Protein Atlas website. The images were analyzed using ImageJ software. The results showed that Cul3 was elevated in tumor tissues compared with normal bile duct tissues (Fig. 4C). Moreover, survival analysis was performed to evaluate the correlation between

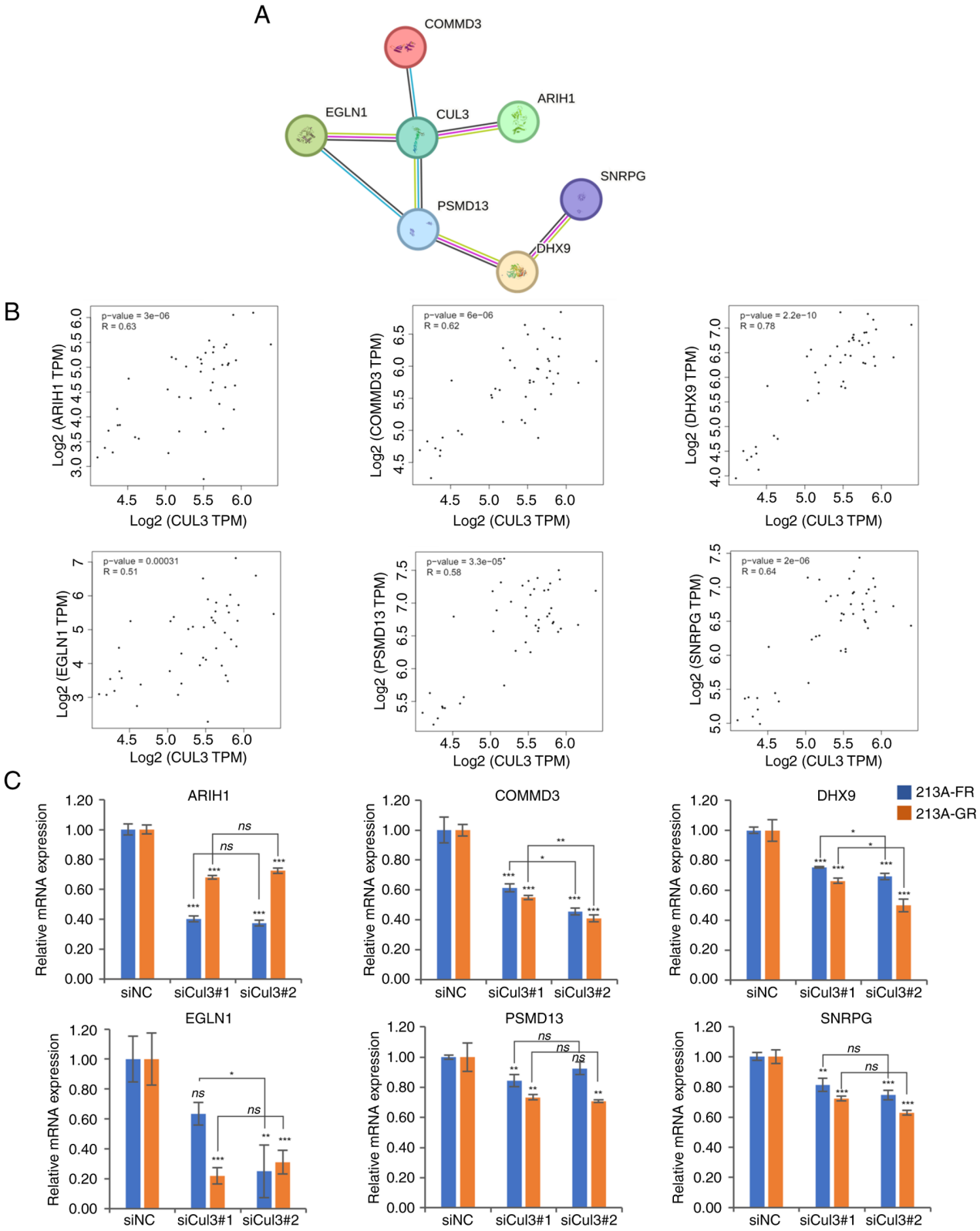

Figure 5. Cul3 correlated genes. (A) STRING analysis of proteins upregulated in drug-resistant CCA cells revealed the Cul3 protein-protein interaction network. (B) Correlation analyses between Cul3 and potential Cul3 correlated genes in tissues of patients with CCA based on TCGA data. (C) mRNA expression of six potential Cul3 partners, namely *ARIH1, COMMD3, DHX9, EGLN1, PSM13* and *SNRPG* analyzed in Cul3 knockdown cells. *P<0.05, **P<0.01 and ***P<0.001 siNC- vs. siCul3-transfected groups. Cul3, cullin 3; CCA, cholangiocarcinoma; STRING, The Search Tool for the Retrieval of Interacting Genes/Proteins; TCGA, The Cancer Genome Atlas; si, short interfering; NC, negative control; ns, not significant.

Cul3 expression and overall as well as disease-free survival time of the patients. However, no significant correlation was found (Fig. 4D).

Cul3 and its correlated genes in CCA. To identify genes correlated with Cul3, a list of upregulated proteins in KKU-213A-FR and KKU-213A-GR cell lines was obtained

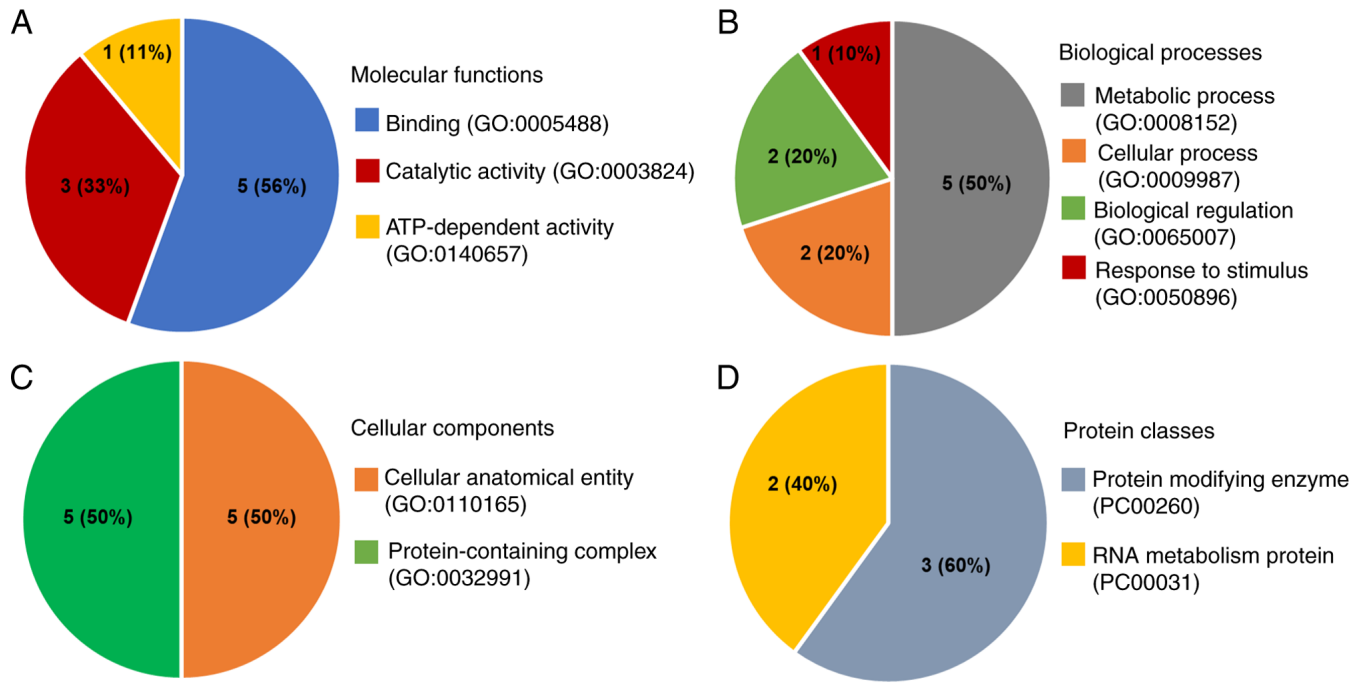

Figure 6. GO analysis of Cul3 and its correlated genes. The genes were categorized through the PANTHER classification system using GO annotations. The categories are: (A) Molecular function, (B) Biological processes, (C) Cellular components and (D) Protein classes. GO, Gene Ontology.

from the ProteomeXchange Consortium via the jPOST partner repository with the data set identifier JPST002506 and PXD049309 (https://proteomecentral.proteomexchange.org/cgi/GetDataset?ID=PXD049309) and uploaded into the STRING analysis platform version 12.0. The results showed that six proteins, including COMMD3, ARIH1, EGLN1, PSMD13, DHX9 and SNRPG, form a highly interactive network with Cul3 (Fig. 5A). In addition, the correlation between these genes and Cul3 in the tissues of patients with CCA was further explored using TCGA data through the GEPIA2 web portal. The correlation analysis revealed that the mRNA expression of these genes positively correlated with Cul3 expression (Fig. 5B). Furthermore, the mRNA expression of six genes was measured in Cul3 knockdown cells. The RT-qPCR results showed that Cul3 knockdown significantly suppressed the expression of *ARIH1*, *COMMD3*, *DHX9 and SNRPG* (Fig. 5C and Table SIV). In KKU-213A-GR cells, both *EGLN1* and *PSMD13* were significantly suppressed by either siCul3#1 or siCul3#2. In KKU-213A-FR cells, *EGLN1* was significantly suppressed only by siCul3#2, while *PSMD13* was significantly suppressed only by siCul3#1.

GO analysis. Cul3 and its correlated genes were further categorized based on their molecular functions, biological processes, cellular components and protein classes using the GO database through the PANTHER classification system. When categorized by molecular function, the largest fraction (56%) belonged to the binding category, including Cul3, ARIH1, DHX9, EGLN1 and SNRPG, followed by catalytic activity (33%) and ATP-dependent activity (11%; Fig. 6A). Biological process ontology indicated that the majority of the proteins were involved in metabolic processes (50%), including Cul3, ARIH1, EGLN1, PSMD13 and SNRPG, followed by cellular processes (20%), biological regulation (20%) and response to stimuli (10%; Fig. 6B). Proteins were classified based on cellular components into two groups: Cellular anatomical entities (50%), including ARIH1, DHX9, EGLN1, PSMD13 and SNRPG and protein-containing complexes (50%), including Cul3, ARIH1, DHX9, PSMD13 and SNRPG (Fig. 6C). Lastly, protein classes showed two groups: Protein-modifying enzymes (60%; including Cul3, ARIH1, PSMD13) and RNA metabolism proteins (40%; including DHX9 and SNRPG) (Fig. 6D). The findings of the KEGG pathway analysis indicated that no significant enrichment was identified in the KEGG pathway (Table SV). The observed outcome was influenced by the limited number of input genes.

Discussion

Due to late diagnosis and limited treatment options, the median survival rate for patients with advanced CCA is <1 year, even when treated with a combination of chemotherapeutic drugs (7-9). Tumor recurrence due to drug resistance remains a major challenge in CCA treatment. Our research group previously identified DEPs in drug-resistant cell lines (KKU-213A-FR and KKU-213A-GR) compared with the parental cell line (KKU-213A), among which Cul3 was one of the most upregulated proteins identified.

Cul3 is a component of the CRL3 complex, essential for the protein ubiquitination process. CRLs consist of four main components: A Cullin protein (Cul), a RING-finger protein, an adaptor protein and a substrate receptor protein (15). The C-terminal end of the Cul protein connects to the RING-finger protein, which recruits the E2 enzyme with ubiquitin. The N-terminal end of the Cul protein binds with the adaptor protein, which in turn binds to the specific target protein. Once the target protein binds with the adaptor, the E2 enzyme

transfers ubiquitin to the target protein, leading to its degradation by the proteasome (32).

Specific substrate adapters influence various biochemical and cellular functions, including protein degradation, cell cycle regulation, cell division, DNA damage repair and epigenetic regulation (33-35). Cul3 plays a dual role in cancer development, both supporting and suppressing cancer progression. For instance, high Cul3 expression is associated with late-stage breast cancer (36), where it ubiquitinates the breast cancer metastasis suppressor 1 protein, which is implicated in suppressing metastasis (16). Similarly, Cul3 upregulation has been observed in aggressive metastatic bladder cancer (17).

Conversely, Cul3 expression suppresses tumor progression in ovarian cancer (37) and lung adenocarcinoma (19,38). Some studies have shown that increased Cul3 expression enhances chemosensitivity both *in vitro* and *in vivo* (37), leading to a favorable prognosis for patients (19). Dorr *et al* (38) demonstrated that Cul3 upregulation inhibits cell proliferation, colony formation and migration of lung adenocarcinoma cell lines.

The role of Cul3 in CCA is limited and multifaceted. A study by Feng *et al* (39) found that Cul3 mutations primarily promote cancer progression by modifying the immune microenvironment. CCA with low Cul3 expression shows increased sensitivity to chemotherapy and targeted therapies, suggesting new treatment approaches for CCA. This finding aligns with our study, which discovered that Cul3 is elevated in drug-resistant CCA cells and upregulated in CCA tumor tissues. *In vitro* suppression of Cul3 expression attenuated the aggressive phenotypes of CCA cells. Conversely, another study revealed that Cul3 acts as a tumor suppressor gene. Cul3 deficiency increases Nrf2 and Cyclin D1 protein levels, leading to cholangiocyte expansion and CCA initiation. It also boosts Cxcl9 secretion in stromal cells, attracting T cells and raises Amphiregulin (Areg) production via Nrf2, causing liver inflammation. This inflammation promotes the accumulation of exhausted $PD1^{high}$ CD8 T cells, reducing their cytotoxic activity and enabling CCA progression (40). These discrepancies suggest a complex role for Cul3 in CCA and indicate the need for further validation.

The present proteomics study revealed that Cul3 was upregulated in both 5-FU and gemcitabine-resistant cell lines. The present study, confirmed Cul3 upregulation at both mRNA and protein levels in KKU-213A-FR and KKU-213A-GR compared with their parental cell line. In addition, results from the UALCAN web portal and The Human Protein Atlas indicated high Cul3 expression in CCA patient tissues. The limitation of the present study is the lack of comparison between Cul3 expression in chemosensitive and chemoresistant CCA patient samples. Future research analyzing Cul3 expression in these samples will help to emphasize the clinical relevance of Cul3 in CCA.

The present study performed *in vitro* loss-of-function studies using siRNAs to investigate the role of Cul3 in drug-resistant cell lines. The results confirmed the involvement of Cul3 in drug resistance development, showing that suppressing Cul3 expression enhanced chemosensitivity in drug-resistant cell lines. Furthermore, Cul3 knockdown reduced the growth rate and induced cell cycle arrest at the G_0/G_1 phases by reducing cyclin D, CDK4 and CDK6, which are G_1 phase regulatory proteins. The results underscored the oncogenic role of Cul3 in CCA, aligning with previous research in bladder cancer, breast cancer and nasopharyngeal carcinoma, where silencing Cul3 decreased cell proliferation and induced cell cycle arrest (17,41,42). The present study also showed that Cul3 silencing reduced the number of migrated and invaded cells in drug-resistant CCA cells, indicating that Cul3 plays a significant role in supporting cancer cell motility. The findings of the present study are consistent with those in bladder cancer (17) and nasopharyngeal carcinoma (42), where suppressing Cul3 reduced metastasis abilities.

STRING analysis using a list of DEPs in KKU-213A-FR and KKU-213A-GR from proteomics results revealed a protein network including Cul3 and six other proteins: ARIH1, COMMD3, DHX9, EGLN1, PSMD13 and SNRPG. These proteins have been shown in previous studies to act as oncogenic factors in human cancers. ARIH1 promotes metastasis through epithelial-mesenchymal transition (EMT) in breast cancer by binding to cullin-RBX1 complexes, leading to the degradation of Poly(rC)-binding protein 1 (PCBP1) (43). COMMD3 regulates CRL by preventing the binding of Cullin-associated Nedd8-dissociated protein 1, promoting ubiquitination of various targets and has been linked to poor prognosis in metastatic prostate cancer (44,45). PSMD13, a regulator subunit of the 26S proteasome, has been linked to the maintenance of stemness and EMT processes in hepatocellular carcinoma (46). EGLN1, a cellular oxygen sensor, promotes tumor development and radiotherapy resistance in nasopharyngeal carcinoma by facilitating p53 ubiquitination (47). DHX9 regulates RNA and DNA processes and its dysregulation can contribute to tumorigenesis by mediating the binding of the EGFR to target gene promoters, stimulating cyclin D1 transcription and promoting proliferation (48). SNRPG is a component of the spliceosome and its dysregulation can lead to aberrant splice variants contributing to oncogenesis and tumor progression (49).

The protein-protein interaction network from STRING analysis revealed potential key novel proteins involved in the development and drug resistance of CCA. Gene expression analysis using GEPIA2 also showed a positive correlation between Cul3 and all six genes in the network. In addition, RT-qPCR revealed that Cul3 knockdown significantly suppressed the mRNA expression of these six genes, suggesting that Cul3 may regulate the expression or function of these downstream target genes.

GO analysis of Cul3 and its correlated genes revealed a multifaceted role of these proteins in CCA cells. The categorization by molecular function indicated that a significant portion of these proteins were involved in binding activities, followed by those involved in catalytic activity and ATP-dependent activity. This finding underscored the diverse interactions and functional roles these proteins play in cellular processes, particularly in cancer cell metabolism and signaling pathways (50). Furthermore, the biological process ontology highlighted that the majority of these proteins participated in metabolic processes, a critical aspect of cancer cell proliferation and survival, with the remaining involved in cellular processes, biological regulation and response to stimuli. This was consistent with existing literature suggesting that metabolic reprogramming is a hallmark of cancer (51). The classification by cellular components divided these proteins into two equal groups: Cellular anatomical entities and protein-containing complexes, indicating their structural

and functional diversity within the cellular environment (52). Lastly, the protein class categorization revealed a split between protein-modifying enzymes and RNA metabolism proteins. This is particularly relevant in the context of cancer, where protein modification and RNA metabolism are crucial for the regulation of gene expression and cellular adaptation to stress (53-55). Overall, these GO analyses provide a broader understanding of the functional landscape of Cul3 and its correlated genes in CCA, highlighting potential targets for therapeutic intervention. The involvement of these proteins in key cellular processes and their diverse molecular functions underline the complexity of cancer biology and the necessity for targeted therapeutic strategies.

In conclusion, the present study demonstrated the aberrant expression of Cul3 in both drug-resistant CCA cells and CCA patient tissues. Suppression of Cul3 expression sensitizes CCA cells to chemotherapeutic drugs, slows cancer cell growth, reduces colony formation, induces cell cycle arrest and decreases cell motility. However, the present study lacked functional rescue experiments. Future research should include the overexpression of Cul3 in Cul3-low expressing cell lines using overexpression plasmids to further elucidate its role. In addition, the present study did not investigate the role of Cul3 in animal models. Future research should use Cul3-stable knockdown or Cul3-stable overexpressing cell lines to study tumor growth through a xenograft model and to investigate the role of Cul3 in metastasis through experimental metastasis models using NOD/SCID mice. Further investigations into the function and association between Cul3 and its correlated genes may help identify novel therapeutic targets for drug-resistant CCA in the future.

Acknowledgements

Not applicable.

Funding

The present study was supported by the National Science, Research and Innovation Fund (NSRF) and Prince of Songkla University (grant no. SCI6801097S) to SO. KP was supported by a Graduate Fellowship (Research Assistant), Faculty of Science, Prince of Songkla University, contract no. 1-2565-02-023. PT was supported by a Prince of Songkla University-Ph.D. Scholarship (grant no. PSU_PHD2565-002).

Availability of data and materials

The data generated in the present study are included in the figures and/or tables of this article.

Authors' contributions

SO, KP, SR, PR and SS conceived and designed the study. KP, KK and PT performed the experiments collected and analyzed the data, produced the figures and wrote the manuscript. SO, KK, KP, SR, PR and SS performed bioinformatics and statistical analysis. SO, SR, PR and SS confirm the authenticity of all the raw data and revised the manuscript. All authors read and approved the final manuscript.

Ethics approval and consent to participate

Not applicable.

Patient consent for publication

Not applicable.

Competing interests

The authors declare that they have no competing interests.

References

1. Kirstein MM and Vogel A: Epidemiology and risk factors of cholangiocarcinoma. Visc Med 32: 395-400, 2016.
2. Blechacz B: Cholangiocarcinoma: Current knowledge and new developments. Gut Liver 11: 13-26, 2017.
3. Kodali S, Connor AA, Brombosz EW and Ghobrial RM: Update on the screening, diagnosis, and management of cholangiocarcinoma. Gastroenterol Hepatol (N Y) 20: 151-158, 2024.
4. Bertuccio P, Malvezzi M, Carioli G, Hashim D, Boffetta P, El-Serag HB, La Vecchia C and Negri E: Global trends in mortality from intrahepatic and extrahepatic cholangiocarcinoma. J Hepatol 71: 104-114, 2019.
5. Adeva J, Sangro B, Salati M, Edeline J, La Casta A, Bittoni A, Berardi R, Bruix J and Valle JW: Medical treatment for cholangiocarcinoma. Liver Int 39 (Suppl 1): S123-S142, 2019.
6. Rizvi S and Gores GJ: Pathogenesis, diagnosis and management of cholangiocarcinoma. Gastroenterology 145: 1215-1229, 2013.
7. Neoptolemos JP, Moore MJ, Cox TF, Valle JW, Palmer DH, McDonald AC, Carter R, Tebbutt NC, Dervenis C, Smith D, *et al*: Effect of adjuvant chemotherapy with fluorouracil plus folinic acid or gemcitabine vs observation on survival in patients with resected periampullary adenocarcinoma: The ESPAC-3 periampullary cancer randomized trial. JAMA 308: 147-156, 2012.
8. Okusaka T, Nakachi K, Fukutomi A, Mizuno N, Ohkawa S, Funakoshi A, Nagino M, Kondo S, Nagaoka S, Funai J, *et al*: Gemcitabine alone or in combination with cisplatin in patients with biliary tract cancer: A comparative multicentre study in Japan. Br J Cancer 103: 469-474, 2010.
9. Valle J, Wasan H, Palmer DH, Cunningham D, Anthoney A, Maraveyas A, Madhusudan S, Iveson T, Hughes S, Pereira SP, *et al*: Cisplatin plus gemcitabine versus gemcitabine for biliary tract cancer. N Engl J Med 362: 1273-1281, 2010.
10. Fouassier L, Marzioni M, Afonso MB, Dooley S, Gaston K, Giannelli G, Rodrigues CMP, Lozano E, Mancarella S, Segatto O, *et al*: Signalling networks in cholangiocarcinoma: Molecular pathogenesis, targeted therapies and drug resistance. Liver Int 39: 43-62, 2019.
11. Sarikas A, Hartmann T and Pan ZQ: The cullin protein family. Genome Biol 12: 220, 2011.
12. Kamitani T, Kito K, Nguyen HP and Yeh ET: Characterization of NEDD8, a developmentally down-regulated ubiquitin-like protein. J Biol Chem 272: 28557-28562, 1997.
13. Zhang S, Yu Q, Li Z, Zhao Y and Sun Y: Protein neddylation and its role in health and diseases. Signal Transduct Target Ther 9: 85, 2024.
14. Wang P, Song J and Ye D: CRL3s: The BTB-CUL3-RING E3 ubiquitin ligases. Adv Exp Med Biol 1217: 211-223, 2020.
15. Cheng J, Guo J, Wang Z, North BJ, Tao K, Dai X and Wei W: Functional analysis of Cullin 3 E3 ligases in tumorigenesis. Biochim Biophys Acta Rev Cancer 1869: 11-28, 2018.
16. Kim B, Nam HJ, Pyo KE, Jang MJ, Kim IS, Kim D, Boo K, Lee SH, Yoon JB, Baek SH and Kim JH: Breast cancer metastasis suppressor 1 (BRMS1) is destabilized by the Cul3-SPOP E3 ubiquitin ligase complex. Biochem Biophys Res Commun 415: 720-726, 2011.
17. Grau L, Luque-Garcia JL, González-Peramato P, Theodorescu D, Palou J, Fernandez-Gomez JM and Sánchez-Carbayo M: A quantitative proteomic analysis uncovers the relevance of CUL3 in bladder cancer aggressiveness. PLoS One 8: e53328, 2013.
18. Yuan WC, Lee YR, Huang SF, Lin YM, Chen TY, Chung HC, Tsai CH, Chen HY, Chiang CT, Lai CK, *et al*: A Cullin3-KLHL20 ubiquitin ligase-dependent pathway targets PML to potentiate HIF-1 signaling and prostate cancer progression. Cancer Cell 20: 214-228, 2011.

19. Zhou J, Zhang S, Xu Y, Ye W, Li Z, Chen Z and He Z: Cullin 3 overexpression inhibits lung cancer metastasis and is associated with survival of lung adenocarcinoma. Clin Exp Metastasis 37: 115-124, 2020.
20. Kerdkumthong K, Roytrakul S, Songsurin K, Pratummanee K, Runsaeng P and Obchoei S: Proteomics and bioinformatics identify drug-resistant-related genes with prognostic potential in cholangiocarcinoma. Biomolecules 14: 969, 2024.
21. Wattanawongdon W, Hahnvajanawong C, Namwat N, Kanchanawat S, Boonmars T, Jearanaikoon P, Leelayuwat C, Techasen A and Seubwai W: Establishment and characterization of gemcitabine-resistant human cholangiocarcinoma cell lines with multidrug resistance and enhanced invasiveness. Int J Oncol 47: 398-410, 2015.
22. Kerdkumthong K, Chanket W, Runsaeng P, Nanarong S, Songsurin K, Tantimetta P, Angsuthanasombat C, Aroonkesorn A and Obchoei S: Two recombinant bacteriocins, rhamnosin and lysostaphin, show synergistic anticancer activity against gemcitabine-resistant cholangiocarcinoma cell lines. Probiotics Antimicrob Proteins 16: 713-725, 2024.
23. Johansson C, Samskog J, Sundström L, Wadensten H, Björkesten L and Flensburg J: Differential expression analysis of *Escherichia coli* proteins using a novel software for relative quantitation of LC-MS/MS data. Proteomics 6: 4475-4485, 2006.
24. Thorsell A, Portelius E, Blennow K and Westman-Brinkmalm A: Evaluation of sample fractionation using micro-scale liquid-phase isoelectric focusing on mass spectrometric identification and quantitation of proteins in a SILAC experiment. Rapid Commun Mass Spectrom 21: 771-778, 2007.
25. Livak KJ and Schmittgen TD: Analysis of relative gene expression data using real-time quantitative PCR and the 2(-delta delta C(T)) method. Methods 25: 402-408, 2001.
26. Chandrashekar DS, Karthikeyan SK, Korla PK, Patel H, Shovon AR, Athar M, Netto GJ, Qin ZS, Kumar S, Manne U, *et al*: UALCAN: An update to the integrated cancer data analysis platform. Neoplasia 25: 18-27, 2022.
27. Tang Z, Kang B, Li C, Chen T and Zhang Z: GEPIA2: An enhanced web server for large-scale expression profiling and interactive analysis. Nucleic Acids Res 47: W556-W560, 2019.
28. Pontén F, Jirström K and Uhlen M: The Human Protein Atlas-a tool for pathology. J Pathol 216: 387-393, 2008.
29. Szklarczyk D, Gable AL, Nastou KC, Lyon D, Kirsch R, Pyysalo S, Doncheva NT, Legeay M, Fang T, Bork P, *et al*: The STRING database in 2021: Customizable protein-protein networks and functional characterization of user-uploaded gene/measurement sets. Nucleic Acids Res 49: D605-D612, 2021.
30. Mi H, Muruganujan A, Ebert D, Huang X and Thomas PD: PANTHER version 14: More genomes, a new PANTHER GO-slim and improvements in enrichment analysis tools. Nucleic Acids Res 47: D419-D426, 2019.
31. Ge SX, Jung D and Yao R: ShinyGO: A graphical gene-set enrichment tool for animals and plants. Bioinform 36: 2628-2629, 2020.
32. Bulatov E and Ciulli A: Targeting Cullin-RING E3 ubiquitin ligases for drug discovery: Structure, assembly and small-molecule modulation. Biochem J 467: 365-386, 2015.
33. Chen RH: Cullin 3 and its role in tumorigenesis. Adv Exp Med Biol 1217: 187-210, 2020.
34. Genschik P, Sumara I and Lechner E: The emerging family of CULLIN3-RING ubiquitin ligases (CRL3s): Cellular functions and disease implications. EMBO J 32: 2307-2320, 2013.
35. Chen HY and Chen RH: Cullin 3 ubiquitin ligases in cancer biology: Functions and therapeutic implications. Front Oncol 6:113, 2016.
36. Haagenson KK, Tait L, Wang J, Shekhar MP, Polin L, Chen W and Wu GS: Cullin-3 protein expression levels correlate with breast cancer progression. Cancer Biol Ther 13: 1042-1046, 2012.
37. Dong M, Qian M and Ruan Z: CUL3/SPOP complex prevents immune escape and enhances chemotherapy sensitivity of ovarian cancer cells through degradation of PD-L1 protein. J Immunother Cancer 10: e005270, 2022.
38. Dorr C, Janik C, Weg M, Been RA, Bader J, Kang R, Ng B, Foran L, Landman SR, O'Sullivan MG, *et al*: Transposon mutagenesis screen identifies potential lung cancer drivers and CUL3 as a tumor suppressor. Mol Cancer Res 13: 1238-1247, 2015.
39. Feng Y, Zhao M, Wang L, Li L, Lei JH, Zhou J, Chen J, Wu Y, Miao K and Deng CX: The heterogeneity of signaling pathways and drug responses in intrahepatic cholangiocarcinoma with distinct genetic mutations. Cell Death Dis 15: 34, 2024.
40. Zhao M, Quan Y, Zeng J, Lyu X, Wang H, Lei JH, Feng Y, Xu J, Chen Q, Sun H, *et al*: Cullin3 deficiency shapes tumor microenvironment and promotes cholangiocarcinoma in liver-specific Smad4/Pten mutant mice. Int J Biol Sci 17: 4176-4191, 2021.
41. Li X, Yang KB, Chen W, Mai J, Wu XQ, Sun T, Wu RY, Jiao L, Li DD, Ji J, *et al*: CUL3 (cullin 3)-mediated ubiquitination and degradation of BECN1 (beclin 1) inhibit autophagy and promote tumor progression. Autophagy 17: 4323-4340, 2021.
42. Zeng R, Tan G, Li W and Ma Y: Increased expression of cullin 3 in nasopharyngeal carcinoma and knockdown inhibits proliferation and invasion. Oncol Res 26: 111-122, 2018.
43. Howley BV, Mohanty B, Dalton A, Grelet S, Karam J, Dincman T and Howe PH: The ubiquitin E3 ligase ARIH1 regulates hnRNP E1 protein stability, EMT and breast cancer progression. Oncogene 41: 1679-1690, 2022.
44. Mao X, Gluck N, Chen B, Starokadomskyy P, Li H, Maine GN and Burstein E: COMMD1 (copper metabolism MURR1 domain-containing protein 1) regulates Cullin RING ligases by preventing CAND1 (Cullin-associated Nedd8-dissociated protein 1) binding. J Biol Chem 286: 32355-32365, 2011.
45. Zhu T, Peng X, Cheng Z, Gong X, Xing D, Cheng W and Zhang M: COMMD3 expression affects angiogenesis through the HIF1α/VEGF/NF-κB signaling pathway in hepatocellular carcinoma in vitro and in vivo. Oxid Med Cell Longev 2022: 1655502, 2022.
46. Huang W, Mei J, Liu YJ, Li JP, Zou X, Qian XP and Zhang Y: An analysis regarding the association between proteasome (PSM) and hepatocellular carcinoma (HCC). J Hepatocell Carcinoma 10: 497-515, 2023.
47. Sun L, Wu C, Ming J, Guo E, Zhang W, Li L and Hu G: EGLN1 induces tumorigenesis and radioresistance in nasopharyngeal carcinoma by promoting ubiquitination of p53 in a hydroxylase-dependent manner. J Cancer 13: 2061-2073, 2022.
48. Gulliver C, Hoffmann R and Baillie G: The enigmatic helicase DHX9 and its association with the hallmarks of cancer. Future Sci OA 7: FSO650, 2020.
49. Bielli P, Pagliarini V, Pieraccioli M, Caggiano C and Sette C: Splicing dysregulation as oncogenic driver and passenger factor in brain tumors. Cells 9: 10, 2019.
50. Mi H, Muruganujan A, Casagrande JT and Thomas PD: Large-scale gene function analysis with the PANTHER classification system. Nat Protoc 8: 1551-1566, 2013.
51. Hanahan D and Weinberg RA: Hallmarks of cancer: The next generation. Cell 144: 646-674, 2011.
52. Thomas PD: The Gene Ontology and the meaning of biological function. Methods Mol Biol 1446: 15-24, 2017.
53. Esteve-Puig R, Bueno-Costa A and Esteller M: Writers, readers and erasers of RNA modifications in cancer. Cancer lett 474: 127-137, 2020.
54. Hu H, Hu W, Guo AD, Zhai L, Ma S, Nie HJ, Zhou BS, Liu T, Jia X, Liu X, *et al:* Spatiotemporal and direct capturing global substrates of lysine-modifying enzymes in living cells. Nat Commun 15: 1465, 2024.
55. Wilkinson E, Cui YH and He YY: Context-dependent roles of RNA modifications in stress responses and diseases. Int J Mol Sci 22: 1949, 2021.